

## Elise plans and progress

J.W. Kwan<sup>a</sup>, R.O. Bangerter<sup>a</sup>, A. Faltens<sup>a</sup>, E.P. Lee<sup>a</sup>, C. Peters<sup>a</sup>, L.L. Reginato<sup>a</sup>,  
J.J. Barnard<sup>b</sup>, W.M. Sharp<sup>b</sup>,

<sup>a</sup>Lawrence Berkeley National Laboratory, 1 Cyclotron Road, Berkeley, CA 94720, USA

<sup>b</sup>Lawrence Livermore National Laboratory, Livermore, CA 94550, USA

### Abstract

Elise is a heavy-ion induction linear accelerator that will demonstrate beam manipulations required in a driver for inertial fusion energy. With a line charge density similar to that of heavy-ions drivers, Elise will accelerate a beam pulse (duration of 1  $\mu$ s or more) of  $K^+$  ions from an initial energy of 2 MeV to a final energy 5 MeV or more. In the present design, the Elise electrostatic quadrupoles (ESQs) will have an aperture of radius 2.33 cm operating at  $\pm 59$  kV. The half-lattice periods range from 21 to 31 cm. The entire machine will be approximately 30 m long, half of which is the induction accelerator with the remaining half being the injector (including the Marx generator) and the matching section. Elise will be built in a way that allows future expansion into the full Induction Linear Accelerator Systems Experiments (ILSE) configuration, so it will have an array of four ESQ focusing channels capable of transporting up to a total of 3.2 A of beam current. Elise will also have an active alignment system with an alignment tolerance of less than 0.1 mm. Initially, only one beam channel will be used during nominal Elise operation. At the currently expected funding rate, the construction time will be 4.75 years, with FY95 being an extra year for research and development before construction. Total project cost is estimated to be US\$25.9m, including contingency costs.

### 1. Introduction

The main driver approach of the US heavy-ion fusion program is to accelerate multiple beams using induction technology for a linear accelerator (LINAC) or recirculating configuration. The standard multi-beam induction accelerator system, as shown in Fig. 1, consists of components such as ion sources, injectors, matching sections, an acceleration section with electric focusing, beam combiners, an acceleration section with magnetic focusing, drift compression lines, and a final focusing system. Electrostatic focusing is

more effective than magnetic focusing at the front end of the machine, because of low ion velocity. The initial beam current of 1 A per beam is based on beam transport considerations and is not limited by the ion sources. The final particle energy and beam current delivered to the target are of the order of 10 GeV and 4 kA per beam. To reach such high currents, multiple beams undergo pulse compression in time by a factor of  $10^3$  from an initial beam with 1 A and 10  $\mu$ s, down to about 10 ns. An additional factor of 4 increase in current is realized by combining four beams into one

at about 100 MeV. As a result of intrinsically low impedance, an induction accelerator has the advantage of being able to accelerate large beam currents with high power efficiency. For economical reasons, a fusion driver should have a repetition rate of 3–10 Hz and a lifetime of about 30 years. At a duty factor of 65%, the total number of pulses is about  $3 \times 10^9$ .

Lawrence Berkeley National Laboratory (LBNL), in collaboration with Lawrence Livermore National Laboratory (LLNL) and industrial partners, has proposed the induction LINAC systems experiments (ILSE) to study the beam dynamics issues and develop the technology of heavy-ions induction drivers. ILSE's full capability can be summarized as follows (the last four items are downstream experiments using the output beam from ILSE):

- (i) inductive acceleration using either electric or magnetic focusing;
- (ii) beam combining with limited emittance growth;
- (iii) beam pulse shaping and longitudinal control;
- (iv) accelerator alignment and beam steering;
- (v) demonstrating the accelerator technology and the associated cost;
- (vi) magnetic bending of a space-charge-dominated ion beam;
- (vii) drift-compression current amplification;
- (viii) final focusing experiments, with or without space-charge neutralization;
- (ix) induction recirculator experiments.

Comparing previous induction LINAC experimental test beds with the parameters of a fusion driver, ILSE appears as the next logical step in the inertial fusion energy (IFE) program plan. Table 1 shows the parameters of the single-beam transport experiment (SBTE) [1] performed at LBNL between 1981 and 1985, the multiple-beam experiment (MBE-4) [2] from 1985 to 1991, the proposed ILSE and a typical driver. To save cost, ILSE will only have a final energy of about 10 MeV; however, the ILSE beams will have a driver-scale line charge density and driver beam radius for studying high intensity, heavy-ion beam physics. The full ILSE configuration has an array of four electrostatic quadrupoles (ESQ) focused

acceleration channels capable of transporting up to a total of 3.2 A of beam current from the injector. The four beams are combined into one before entering the magnetic focusing channels for further acceleration.

The ILSE proposal, originally made in 1988, was revised in 1993 to a reduced cost of about US\$50m on a 4-year construction schedule. As a result of funding limitations, the project is now divided into two stages. The first stage, called Elise, will only contain the electric focused acceleration section and will use an existing single-beam injector. The second stage will include a four-beam injector, a beam combiner and a magnetically focused acceleration section. Elise is estimated to cost \$25.9m, i.e., about half the price of ILSE. The project received Key Decision 1 approval from the US Department of Energy in December 1994. Detail design work will take place in FY96 and the full design and construction period has been elongated to 4.75 years to fit the anticipated funding rate limitation. On completion, Elise will be the largest ion induction accelerator ever built and will be a significant step towards the development of a fusion driver.

## 2. Design requirements

### 2.1. Technical design parameters

The key technical design parameters for Elise are depicted in Table 2. Elise will accelerate the ions from 2 MeV to 5 MeV or more. For Elise to

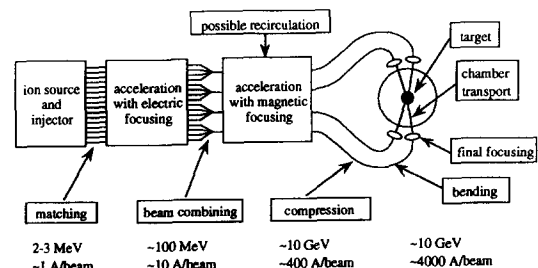


Fig. 1. Block diagram of the standard multi-beam induction accelerator system for a heavy-ion fusion driver. The values of the beam energy and current are rounded-off numbers for magnitude estimation.

Table 1  
Parameters of induction LINAC experiments

	SBTE	MBE-4	Elise/ILSE	Driver
Ion species	Cs <sup>+</sup>	Cs <sup>+</sup>	K <sup>+</sup>	Hg <sup>+</sup>
Number of beams	1	4	4/1	64→16
Final voltage (MV)	0.2	1	5/10	10 000
Initial current per beam (A)	0.020	0.010	0.8/3.2	0.42
Line charge density (μC m <sup>-1</sup> )	0.03	0.01	0.25	0.25
Bunch length (m)	11.0	1.1→0.25	3.14→2.80	25→10
Pulse width (μs)	20	1→0.2	1→0.4	15→0.1

be expandable to ILSE, it will have four beam channels but only a single-beam channel will be in operation, using an existing 2 MeV injector [3]. The injector has demonstrated over 0.8 A of K<sup>+</sup> beam with a normalized beam emittance of less than 1.0 π mm mrad. According to Table 2, a driver-like 3 MeV Hg<sup>+</sup> beam (mass = 200) has a bunch length and pulse length at injection of about 25 m and 15 μs respectively. At 0.42 A of beam current, the corresponding line charge density λ is 0.25 μC m<sup>-1</sup>.

We have chosen to limit the Elise pulse length to less than 2 μs, so that the accelerator length can be kept to within 15 m. The beam leaving the injector is expected to have a rise-plus-fall time totalling more than 0.7 μs, so a pulse length with the flat-top shorter than 1 μs is considered to be not cost effective, based on dollar-per-joule calculation (see Subsection 3.4 and Fig 6 later).

A driver beam must be focusable down to a spot radius of a few millimeters at a target inside a reactor chamber. This focusing capability

is determined by the beam quality at the final focusing stage, i.e. the beam transverse and longitudinal emittance must be adequate at that point. For a convergence angle of 15 mrad and a focal spot radius of 3 mm, the required normalized transverse emittance is 15 π mm mrad or less. If space charge plays a role in the final transport (as a result of insufficient neutralization), then an emittance of 10 π mm mrad or less is required. Scaling the performance of our existing injector to a heavy-ion beam, such as Hg<sup>+</sup>, the injected Hg<sup>+</sup> beam will have a normalized emittance of 0.5 π mm mrad. Thus, the total emittance budget from the injector to the final focus is a factor of 20, but a significant fraction of that will be taken up by emittance growth from merging multiple beams. The percentage of emittance growth in Elise’s acceleration channel depends on the initial emittance

Table 2  
Key technical design parameters for Elise

Initial ion kinetic energy	2 MeV
Initial beam current	0.8 A
Initial pulse duration	1.0 μs
Initial line charge density	0.25 μC m <sup>-1</sup>
Number of beams	1
Final average ion kinetic energy	5 MeV
Final beam energy	4 J
Ion mass number	39 (K <sup>+</sup> ion)
Ion charge state	+1

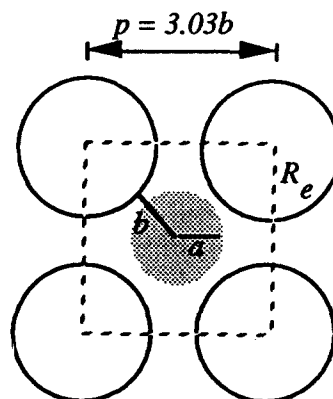


Fig. 2. Cross-sectional view of an ESQ channel.

tance at injection—our aim is to keep Elise's output beam at  $1.0 \pi$  mm mrad or less.

The longitudinal emittance requirement is determined by chromatic aberrations of the final focusing system. In a typical system, the momentum spread  $\delta p/p$  should not exceed 0.5% in final focus. The corresponding energy spread  $\delta T/T$  is 1.0%. Thus, for a beam with 10 GeV and 10 ns, with conventional final focus and transport, the longitudinal emittance ( $\delta T\tau$ ) must be less than 1 eV s.

Elise will have an alignment tolerance of 0.1 mm. Our random error propagation analysis showed that, for 54 half-lattice periods, the accumulation can be up to 20 times the size of individual alignment errors, i.e. 2 mm of beam displacement. Hence, the bore radius must be large enough to accommodate beam displacement of 2 mm without incurring significant beam loss.

Another possible beam loss is caused by collisions with the background gas. The cross-section for  $K^+$  electron loss at an energy of 2 MeV in nitrogen gas is  $4 \times 10^{-16}$  cm<sup>2</sup> (insensitive to beam energy in this energy range). The cross-section for electron capture is five times smaller (and decreases with higher energy) [4]. For a length of 15 m at  $1 \times 10^{-6}$  Torr (room temperature), the beam loss is estimated to be about 2%. We will design Elise to achieve vacuum in the upper  $10^{-7}$  Torr range.

## 2.2. Design optimization

For typical heavy-ion fusion beams, e.g.  $\lambda = 0.25 \mu\text{C m}^{-1}$  at low energy, the space-charge force is very large, so a large quadrupole field is required for beam transport. A major effort in conceptual design has been the cost optimization between transport and acceleration.

The particle energy at which the beam focusing changes from electric to magnetic is determined by comparing the cost of accelerators with ESQs and magnetic quadrupoles. For a heavy-ion fusion driver, superconducting magnetic quadrupoles will be used and the transition takes place at a beam energy of about 100 MeV. Warm-bore magnets must be used because of the presence of many room temperature acceleration gaps. The

requirement of thermal insulation imposes a lower limit on the size of the magnetic quadrupoles. In a typical driver, the magnetic quadrupole aperture radius is about 6 cm [5]. Furthermore, as shown in Subsection 3.1, the optimum ESQ aperture radius is only 2.3 cm (mainly because of the non-linear scaling of electrical breakdown), so it would be economical to combine beamlets from several ESQ channels into a single magnetic quadrupole channel. To keep cost down, we would like to demonstrate magnetic focusing in ILSE at a much lower beam energy, so the limiting factor is our technical capability to construct short, high-quality magnetic quadrupoles with negligible end effects. Our present goal is to make the transition at approximately 5 MeV, where the matched half-lattice period is about 30 cm, using high field pulsed quadrupoles that include some of the design considerations relevant to superconducting quadrupoles.

## 3. Design status

In this section, we discuss some of the key principles used in designing Elise and the characteristics of today's design. More details can be found from the other two papers on the subjects of Elise physics [6] and engineering [7]. Even though the present design has many areas that differ significantly from those described in the conceptual design report (CDR) for ILSE [8] and for Elise [9], many physics and hardware discussions contained in the CDR are still valid.

### 3.1. Optimum current density

For space-charge-dominated beams, the maximum transportable beam current is given as

$$\frac{4QL^2}{\bar{a}^2} = 2(1 - \cos \sigma_0) \quad (1)$$

where  $\bar{a}$  is the mean beam radius,  $\sigma_0$  is the undepressed phase advance per lattice period,  $L$  is the half-lattice period length, and the depressed phase advance is negligibly small for the given emittance [10]. For stable operation,  $\sigma_0$  must stay below  $85^\circ$ . The dimensionless perveance  $Q$  is defined as

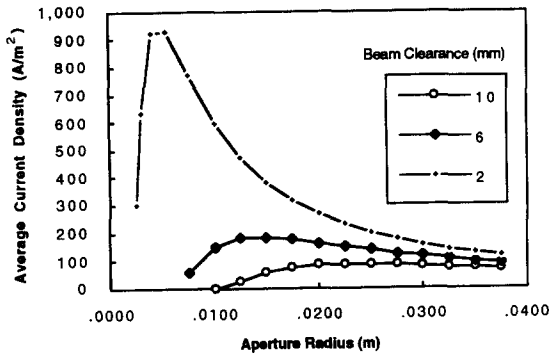


Fig. 3.  $J_{ave}$  as a function of the aperture radius and beam clearance.

$$Q = \frac{2qeI}{(\gamma\beta)^3 mc^3 4\pi\epsilon_0} = \frac{\lambda}{4\pi\epsilon_0 V} \quad (2)$$

where  $q$  is the charge state,  $\gamma$  and  $\beta$  are the relativistic factors, and  $V$  is the accumulated beam voltage. The line charge density  $\lambda$  is therefore given by

$$\lambda = 4\pi\epsilon_0 V \left(\frac{\bar{a}}{2L}\right)^2 2(1 - \cos \sigma_0) \quad (3)$$

For an ESQ with field occupancy factor  $\eta$ , the half-lattice period can be solved using a thick lens approximation [11] as

$$L = b[2(1 - \cos \sigma_0)/\eta^2(1 - 2\eta/3)(V_q/2V)^2]^{1/4} \quad (4)$$

here  $V_q$  is the voltage across the quadrupole electrodes.

An ESQ cross-section is shown in Fig. 2. The aperture radius  $b$  is governed by the equation

$$b = 1.25a + c \quad (5)$$

where  $a$  is the maximum beam radius and  $c$  is the beam clearance (based on an estimate of the beam steering random error and accelerator alignment limits). The coefficient 1.25 arises from a limitation in the image force from the electrodes. The ratio  $a/\bar{a}$  is a function of the quadrupole strength and  $\eta$  [10] and is approximately 1.2–1.3. The electrode radius  $R_e$  is selected to make the dodecapole component of the focusing electric field vanish:  $R_e/b = 1.146 (\approx 8/7)$ .

In an ESQ breakdown test at LBNL [12], we found that the breakdown threshold for the ESQ is proportional to the square root of the spacing

between the quadrupole electrodes, and an ESQ with  $b = 2.2$  cm and  $R_e = 2.53$  cm broke down at 230 kV between the quadrupole electrodes. For a conservative safety margin, we set the normal operating point at 50% or less of the breakdown threshold value.

A useful figure of merit in optimizing the beam current density is the total transported multi-beam current divided by the area occupied by the ESQ array. In our design, the effective length of the ESQ is 6 cm shorter than the physical length of the half-lattice period; hence,  $\eta = (L-6)/L$ . Obviously,  $\eta$  grows with  $L$ ; typical values of  $\eta$  range from 0.71 at the beginning to 0.81 at the end of Elise. In our design, we use Eq. (4) to calculate  $L$  as a function of the aperture radius  $b$  (let  $\sigma_0 = 75^\circ$ ) and adhere to the square-root scaling law for the quadrupole voltage. Using Eq. (5), the beam radius is determined and the transportable beam current is then obtained from Eq. (3). Fig. 3 shows the  $J_{ave}$  values for various beam clearances. For each fixed clearance, there is an optimum aperture radius that produces the maximum average current density. The value of  $J_{ave}$  can be very

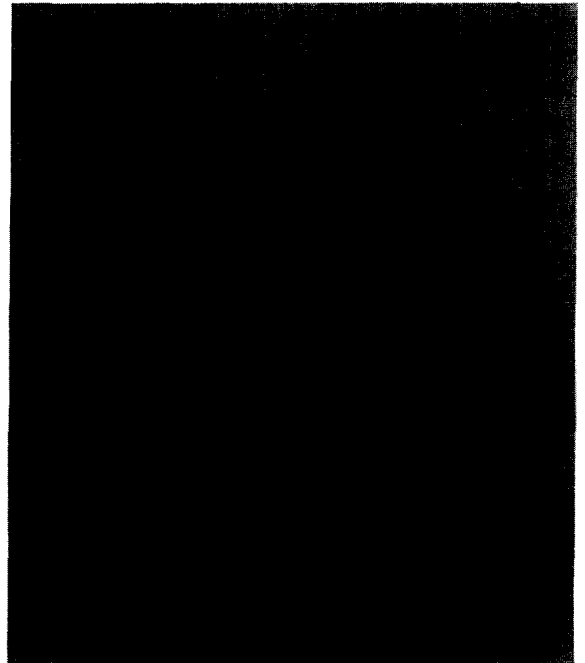


Fig. 4. Picture of the ESQ array.

large for small clearance requirement, which is certainly an opportunity for future system improvement.

In fact, the optimal aperture radius can be derived analytically by assuming that the maximum quadrupole voltage is proportional to  $b^\alpha$ , where  $\alpha$  is typically between 0.5 and 1.0. It can be shown that [5]

$$J_{\text{ave}} = \frac{g(b-c)^2}{b^{3+\alpha}} \quad (6)$$

where  $g$  is some proportional constant. The optimum value of  $b$  is obtained by taking the derivative of the last equation, i.e.

$$b_{\text{opt}} = \frac{(3+\alpha)c}{(1+\alpha)} \quad (7)$$

For  $\alpha = 0.5$  (found in our breakdown test), the optimum aperture radius  $b_{\text{opt}}$  is 2.33 cm for  $c = 1$  cm, and 0.5 cm for  $c = 0.2$  cm.

For Elise we have selected a very conservative beam clearance of 1 cm with an aperture radius of 2.33 cm, and the corresponding ESQ voltage (at 50% breakdown threshold) is 118 kV (or  $\pm 59$  kV w.r.t. ground potential). On successful demonstration of ESQ alignment and beam steering, we can fill the channel with more beam, until the beam radius reaches the clearance limit. For example, with a beam clearance of 2 mm,  $J_{\text{ave}}$  can be as high as 219 A m<sup>-2</sup> and the corresponding line charge density is 0.345  $\mu\text{C m}^{-1}$ .

### 3.2. Matching the beam envelope

In the previous Elise conceptual design [8], the machine used four blocks of acceleration sections and only two different half-lattice period lengths throughout. The advantage of this approach is a possible cost saving in fabricating many parts with the same dimensions. However, the disadvantage is that the mismatch in  $L$  significantly reduces the transportable  $\lambda$ . Elise will be designed with continuously varying half-lattice periods.

At the start, the half-lattice period is 20.8 cm (at 2 MeV with  $\sigma_0 = 75^\circ$ ). As the particles gain energy, a smooth beam envelope can be obtained by matching the envelope angles between lattice periods, i.e.

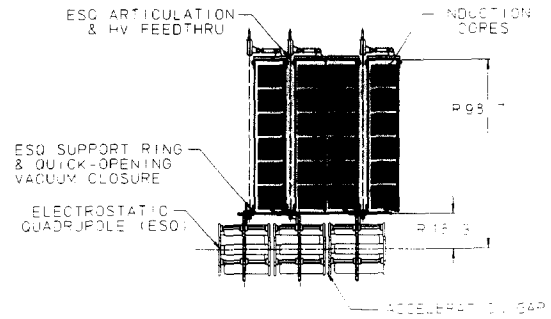


Fig. 5. Schematic diagram of the ESQs and the acceleration modules.

$$\frac{\eta LE'}{V^{1/2}} = \text{constant} \quad (8)$$

Here,  $E$  is the quadrupole field gradient. By keeping the quadrupole voltage and aperture radius constant throughout the machine, the matching condition reduces to a simple matter of keeping the effective length ( $\eta L$ ) proportional to the square root of the particle energy.

By combining Eqs. (4), (5) and (8), and keeping the quadrupole voltage constant, we find that  $\lambda$  is proportional to  $\bar{a}^2(1-2\eta/3)$ . Thus, as  $L$  and  $\eta$  grow (with the beam voltage), the ratio  $a/\bar{a}$  becomes smaller, but  $\sigma_0$  and the transportable  $\lambda$  are reduced. For example, as  $\eta$  changes from 0.71 at the beginning of Elise to 0.81 at the end, the phase advance changes from  $75^\circ$  to  $60^\circ$ , and the transportable  $\lambda$  drops by 10.5%. Although having  $\lambda$  decrease is not the intended schedule for a long driver, it is a match for Elise, because the machine is so short that the bunch length will actually be elongated for most acceleration schedules (including those with pulse compression). For a driver, the acceleration rate is slow, so  $\eta$  increases very slowly towards 1.0. In fact, by enduring a slight mismatch, we can use the simpler scaling of

$$\frac{LE'}{V^{1/2}} = \text{constant} \quad (9)$$

Combining this with Eq. (4), we now find that both  $\sigma_0$  and  $\lambda$  increase with increasing  $\eta$ .

### 3.3. Accelerator hardware

Fig. 4 shows a picture of the ESQ array, and Fig. 5 shows a schematic diagram of the ESQ

structure and the acceleration modules. The ESQ electrodes are mounted on two end-plates that are cantilevered from the middle ground-plate by insulator rods. Each ESQ is kinematically supported and can be articulated for minor alignment adjustment. The gap between the acceleration modules is typically 5 cm; this provides access for the ESQ support ring articulation, high voltage feedthroughs and vacuum pumping.

The basic element of an induction acceleration is the induction core. It is made of many thin layers of magnetic material with insulation in between layers to reduce eddy currents. A core is energized by sending a fast pulse of current through the primary winding. The beam, which forms the secondary ‘winding’, receives an induction voltage equal to the pulser voltage (for a 1:1 winding ratio). Several cores can be electrically energized in parallel, with their induction voltages added in series by the beam. Magnetic materials are available in the form of tapes at standard widths and thicknesses. For example, our present design uses Metglas® tapes 14.2 and 17.0 cm wide and 25.4  $\mu\text{m}$  thick, and mylar insulation 2.5  $\mu\text{m}$  thick. There are also Metglas® tapes 5.1 and 10.2 cm wide available at a higher cost per kilogram. Our goal is to wind these tapes at a packing factor of 75% of Metglas® volume inside the core volume.

An acceleration module is composed of one or more cells axially linked together, and each cell has several layers of induction cores in the radial direction. Initially, the half-lattice period is only long enough for modules with a single cell. At the

high energy end of the accelerator, the half-lattice period becomes long enough to accept acceleration modules that contain double cells. The acceleration module has a metal housing with a small positive gauge pressure of  $\text{SF}_6$ . The purpose of the  $\text{SF}_6$  is to fill the air space inside the module for better voltage holding, so as to improve the packing factor.

Since  $L$  is varying continuously while the module period is quantized (according to the tape width and the number of cells), the two periods do not match. In other words, the intermodule gaps do not always line up at the same place with respect to the ESQ structure, unless we purposely match them up at the expense of introducing extra spacing, so lowering the longitudinal packing factor. To accommodate the physical mismatch, each ESQ is mounted with a unique offset from its support ring. One important design criterion is to avoid the intermodule gaps from lining up against the end-plate and ground-plate regions to allow the voltage feedthroughs to reach the quadrupole electrodes.

Beam acceleration occurs at the gap between end-plates of neighboring ESQs. In designing the lattice, the acceleration voltage is determined by the size of the acceleration module, and the acceleration module is selected according to the available space provided by the half-lattice period.

A pulse forming network (PFN) is used to drive the induction core. As a result of the non-linear magnetic behavior, the pulse current is not constant, so the PFN must have a tapered impedance. The thyratrons (existing surplus units) operate at a nominal voltage of 22.2 kV, delivering 11.1 kV into a matched load. At this voltage, a pulse of 2.5  $\mu\text{s}$  will require a flux change of 0.028 V s per core to avoid saturation. Assuming  $\Delta B = 2$  T, the cross-sectional area of a single 75% packed core is 185  $\text{cm}^2$ .

We will control each of the 51 pulser voltage to within 1% variation, such that the accumulated energy ripple can be less than 0.1%. This can be achieved by using fast correction pulsers on separate small cores, with either an active feedback or feedforward circuit, and applies the correction pulse about once every four or five lattice periods. The ‘ear’ pulses compensate for the space-charge

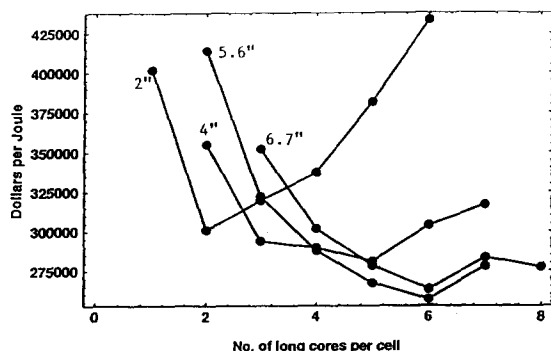


Fig. 6. Cost optimization among various tape widths.

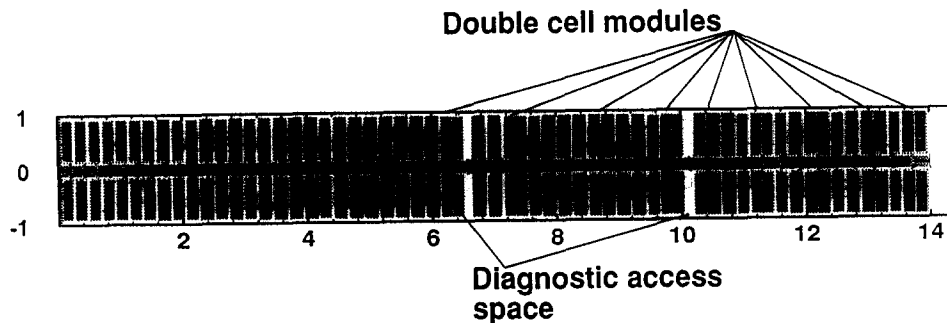


Fig. 7. Elise lattice design.

expansion force at the front and back of a beam bunch. These pulses are of the order of 10 kV for  $0.5 \mu\text{s}$ . The front ear can be generated by using the rising edge of the main acceleration pulse, whereas the back ear must be generated by an additional pulser.

In the original Elise conceptual design, there is a diagnostic section at every eight half-lattice periods (i.e. at the end of each block). The section is normally occupied by 2 ESQs with no acceleration. In performing beam diagnostics, the ESQs will be removed and replaced by diagnostic equipment, such as an emittance scanner. Instead of having these diagnostic stations, the present design has the entire induction section mounted on rails to provide quick access for beam diagnostics and maintenance. A pneumatically operated vacuum closure can remotely disconnect the accelerator at any lattice point.

### 3.4. Cost optimization

There are three major cost factors in an induction linac: the ESQ transport cost (including the vacuum vessel and the ESQ d.c. power supplies); the magnetic material cost; and the pulser cost. The ESQ transport cost is proportional to the number of half-lattice periods in the accelerator. Therefore, from that standpoint, it is more advantageous to maximize the acceleration voltage per gap.

The magnetic material cost is more complicated. For a given flux change, the total cross-sectional area of the cores is fixed, but the volume of magnetic material required depends on the ratio

between the radial dimension and the axial dimension. For a fixed cross-sectional area, the core volume increases with the diameter, so it is more advantageous to minimize the module size to give a lower acceleration voltage per gap. Aside from the cost of raw material and the associated costs of fabrication, housing and support structure, the pulser cost is also proportional to the mass (or volume) of the induction cores, as a result of hysteresis and eddy current loss.

The four most common magnetic materials in use today for induction cores are ferrite, Ni–Fe, silicon steel and Metglas<sup>®</sup> (made by Allied Signals Inc.). Ferrite is good for very short pulses but it has a small  $\Delta B$  value and is too expensive to be considered for a fusion driver. Similarly to ferrite, Ni–Fe is an acceptable material but it is still too expensive for our use. The raw material for silicon steel is inexpensive but it is difficult to make tapes thinner than 0.05 mm. Metglas<sup>®</sup> seems to be the best choice. It is available in thickness of 0.025 mm or less, it has high enough resistivity (and skin depth), and it is reasonably inexpensive. The wider Metglas<sup>®</sup> tapes (14.2 and 17.0 cm) are used by the 60-cycle utility transformer industry, so they are sold at a price 3–4 times lower than the less common narrower (5.01 cm) tapes.

We have used a specialized computer program to examine the cost of various designs, using modules made with different width Metglas<sup>®</sup> tapes and different numbers of cores per cell. Fig. 6 depicts the variable cost of building Elise using various sized modules (not including fixed costs). The cost optimization results can be summarized as follows:

Table 3  
Summary of the present Elise conceptual design

Accelerator outer radius	1 m
Accelerator length	14 m
Number of half-lattice periods	54
Longitudinal packing fraction	68%
Radial packing fraction	75% Metglas <sup>®</sup> core, 63% average
Total flux change	9.25 V s
Half-lattice periods	0.208 → 0.311 m
Occupancy factor	0.71 → 0.81
Initial energy	2 MeV
Initial current pulse length	1.5 $\mu$ s flat-top (=2.5 $\mu$ s voltage)
Final energy (constant current)	5.7 MeV
Final energy (with current amplification)	5.1 MeV/6.8 MeV
Current amplification	1.31
Velocity tilt	15.4%

- (1) the wider tape is more cost-effective (mainly because of a lower raw material cost and a higher packing factor);
- (2) an outer radius of approximately 1 m is the optimum module size, regardless of which Metglas<sup>®</sup> tape width is used in the design;
- (3) using a longer pulse length rather than a higher beam voltage delivers more beam energy downstream (mainly as a result of the fixed rise-and-fall time of the current pulse, and the lower loss from a smaller value of  $dB/dt$ ).

There is an additional advantage in using the transformer-grade (wider) Metglas<sup>®</sup> tapes, in that they would be more uniform and reliable, in both their magnetic and physical properties. It is more than likely that the wider tape is easier to wind than the narrow tape, which had a problem of 'coning' caused by non-uniform tape thickness.

### 3.5. Present design and performance

Based on the optimization results, we have produced an improved conceptual design for Elise. The lattice is shown in Fig. 7. In this design, the half-lattice periods are matched with the beam energy using a constant current acceleration schedule, i.e. square pulses at all gaps and fully utilizing all the available flux change. The final beam energy is 5.7 MeV. By using a different acceleration schedule (trapezoidal pulse shape), the same lattice can compress the current pulse

length from 1.5 to 1.15  $\mu$ s, leading to a 31% current amplification. In this case, the beam head will have 5.1 MeV and the beam tail will have 6.8 MeV (about 15% of velocity tilt).

Among the 54 half-lattice periods, there are two gaps that do not have an acceleration voltage. This occurs because the accumulated module length outruns the accumulated ESQ length. We intend to make use of these two special extra wide gaps for monitoring the beam intensity profile and for vacuum pumping. A summary of the design parameters and performance is shown in Table 3.

## 4. Conclusions

In general, Elise will be designed in such a way that it is compatible with the full ILSE configuration, and the technology employed in Elise should be driver-like, such that the knowledge gained from the project is useful for projecting the costs for a fusion driver. Compared with the earlier conceptual design, the present Elise design has a smaller aperture, variable half-lattice periods, offset ESQ supports, wider Metglas<sup>®</sup> ribbons and a larger module diameter. It produces more than twice as many joules at about the same cost. The emittance diagnostic stations are eliminated, but the machine will be designed for easy disconnection to insert diagnostic equipment. Almost all these changes improve the cost-effectiveness of the machine. The most critical technology issue in the

Elise project is the fabrication of compact low-loss induction cores. Overall, the project is making steady progress and should be completed within the planned budget and schedule.

### Acknowledgments

The authors wish to thank the support of the physics and engineering staff at both LBNL and LLNL Heavy Ion Fusion Programs. This work was supported by the Director, Office of Energy Research, Office of Fusion Energy, US Department of Energy, under Contracts DE-AC03-76SF00098 and W-7405-ENG-48.

### References

- [1] M.G. Tiefenback and D. Keefe, Measurements of stability limits for a space-charge-dominated ion beam in a long A.G. transport channel, Proc. Particle Accelerator Conf., IEEE Trans. Nucl. Sci. NS-32 (1985) 2483.
- [2] T.J. Fessenden, Emittance variations in current-amplifying ion induction linacs, Proc. Particle Accelerator Conf., San Francisco, CA, 6–9 May 1991, p. 586.
- [3] S. Yu., Driver-scale ion injector experiments, paper presented at this symposium.
- [4] R.C. Dehmel, H.K. Chau and H.H. Fleischmann, Experimental stripping cross sections for atoms and ions in gases, 1950–1970, Atomic Data 5 (1973) 231–289.
- [5] R.O. Bangerter, The induction approach to heavy-ion inertial fusion: Accelerator and Target considerations, Proc. Int. Symp. on Heavy Ion Inertial Fusion, Frascati, 25–28 May 1993, Nuovo Cimento (1993) 1445.
- [6] E.P. Lee et al., Physics design and scaling of Elise, Fus. Eng. Des. 32–33 (1996) 323.
- [7] L. Reginato and C. Peters, Engineering research and development for the Elise heavy ion induction accelerator, Fus. Eng. Des. 32–33 (1996) 337.
- [8] ILSE conceptual engineering design study, LBL Pub-5219, Lawrence Berkeley Laboratory, Berkeley, CA, 1989.
- [9] Elise conceptual design report, LBL Pub-5393, Lawrence Berkeley Laboratory, Berkeley, CA, 1994.
- [10] E.P. Lee, The beam envelope equation systematic solution for a periodic quadrupole lattice with space charge, LBL-37050, Lawrence Berkeley Laboratory, Berkeley, CA, April 1995.
- [11] E.P. Lee, Envelope relations, LBNL HIFAR Note 425, Lawrence Livermore National Laboratory, Livermore, CA, 1994.
- [12] P. Seidl and A. Faltens, Electrostatic quadrupoles for heavy-ion fusion, Proc. Particle Accelerator Conf., Washington, DC, 17–20 May 1993.